Advances in Chemical Physics
Stuart A. Rice and Aaron R. Dinner, Series Editors

Advances in Chemical Physics

Volume 153

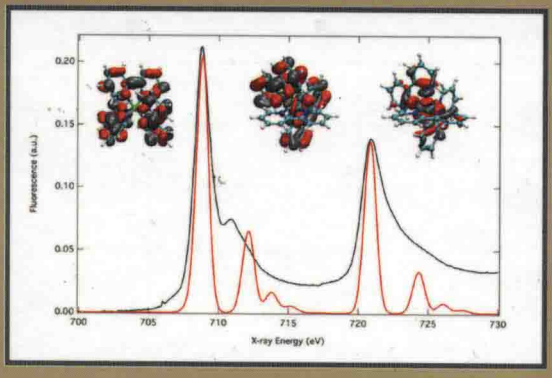

Edited by

Stuart A. Rice and Aaron R. Dinner

WILEY

ADVANCES IN CHEMICAL PHYSICS

VOLUME 153

Edited By

STUART A. RICE

Department of Chemistry
and
The James Franck Institute,
The University of Chicago,
Chicago, Illinois

AARON R. DINNER

Department of Chemistry
and
The James Franck Institute,
The University of Chicago,
Chicago, Illinois

WILEY

Published by John Wiley & Sons, Inc., Hoboken, New Jersey.
Published simultaneously in Canada.

***Library of Congress Catalog Number*:** 58-9935

ISBN: 978-1-118-47786-1

Printed in the United States of America

10 9 8 7 6 5 4 3 2 1

ADVANCES IN CHEMICAL PHYSICS

VOLUME 153

EDITORIAL BOARD

CONTRIBUTORS TO VOLUME 153

MAJED CHERGUI, Ecole Polytechnique Fédérale de Lausanne, Laboratoire de Spectroscopie Ultrarapide, ISIC, FSB-BSP, 1015 Lausanne, Switzerland

LIVIU F. CHIBOTARU, Division of Quantum and Physical Chemistry, Katholieke Universiteit Leuven, Celestijnenlaan 200F, 3001 Leuven, Belgium

WILLIAM T. COFFEY, Department of Electronic and Electrical Engineering, Trinity College, Dublin 2, Ireland

WILLIAM J. DOWLING, Department of Electronic and Electrical Engineering, Trinity College, Dublin 2, Ireland

YURI P. KALMYKOV, Laboratoire de Mathématiques et Physique, Université de Perpignan Via Domitia, 52 Avenue Paul Alduy, 66860 Perpignan Cedex, France

SRIHARI KESHAVAMURTHY, Department of Chemistry, Indian Institute of Technology, Kanpur 208016, India

CHRISTOPHER J. MILNE, Ecole Polytechnique Fédérale de Lausanne, Laboratoire de Spectroscopie Ultrarapide, ISIC, FSB-BSP, 1015 Lausanne, Switzerland

ANDREW MUGLER, FOM Institute AMOLF, Science Park 104, 1098 XG Amsterdam, The Netherlands

THOMAS J. PENFOLD, Ecole Polytechnique Fédérale de Lausanne, Laboratoire de Spectroscopie Ultrarapide, ISIC, FSB-BSP, 1015 Lausanne; Ecole Polytechnique Fédérale de Lausanne, Laboratoire de Chimie et Biochimie Computationnelles, ISIC, FSBBSP, 1015 Lausanne; SwissFEL, Paul Scherrer Institut, 5232 Villigen, Switzerland

ELIZABETH A. PLOETZ, Department of Chemistry, Kansas State University, 213 CBC Building, Manhattan, KS 66506-0401, USA

PAUL E. SMITH, Department of Chemistry, Kansas State University, 213 CBC Building, Manhattan, KS 66506-0401, USA

PIETER REIN TEN WOLDE, FOM Institute AMOLF, Science Park 104, 1098 XG Amsterdam, The Netherlands

SERGUEY V. TITOV, Kotelnikov Institute of Radio Engineering and Electronics of the Russian Academy of Sciences, Vvedenskii Square 1, Fryazino, Moscow Region 141190, Russian Federation

CONTENTS

RECENT ADVANCES IN ULTRAFAST X-RAY ABSORPTION SPECTROSCOPY OF SOLUTIONS

THOMAS J. PENFOLD,[1,2,3] CHRISTOPHER J. MILNE,[1] and MAJED CHERGUI[1]

[1]*Ecole Polytechnique Fédérale de Lausanne, Laboratoire de Spectroscopie Ultrarapide, ISIC, FSB-BSP, 1015 Lausanne, Switzerland*
[2]*Ecole Polytechnique Fédérale de Lausanne, Laboratoire de Chimie et Biochimie Computationnelles, ISIC, FSB-BSP, 1015 Lausanne, Switzerland*
[3]*SwissFEL, Paul Scherrer Institut, 5232 Villigen, Switzerland*

CONTENTS

Advances in Chemical Physics, Volume 153, Second Edition. Edited by Stuart A. Rice and Aaron R. Dinner.

I. INTRODUCTION

The advent of structural techniques such as X-ray, electron and neutron diffraction, nuclear magnetic resonance (NMR), and X-ray absorption spectroscopy (XAS) has made it possible to directly extract the structure of molecules and condensed matter systems, with a strong impact in physics, chemistry, and biology [1–7]. However, the static structure of the systems under study means that often the mechanisms underlying their function are unknown. Thus, from the early days of femtochemistry, efforts were deployed to implement these structural tools in time-domain experiments [8–11]. Since the first implementation of XAS in a pump–probe type experiment [12] in the micro- to millisecond range, time-resolved XAS has emerged as the method of choice for the study of local structural changes of molecules in solution. The wealth of electronic and geometric information available from an X-ray absorption spectrum has led to its implementation for the study of a wide variety of systems [1–7,13–22].

An X-ray absorption spectrum is characterized by absorption edges, which reflect the excitation of core electrons to the ionization threshold and is consequently element specific. For a particular edge, an electron is initially excited to unoccupied or partially filled orbitals just below the ionization potential (IP) giving rise to bound–bound transitions, which form the pre-edge features. This region, thus, yields information about the nature of the unoccupied valence orbitals, as the transition probability is governed primarily by the atomic dipole selection rules. Above the IP, resonances show up due to interferences of the photoelectron wave from the absorbing atom with the wave scattered back from the neighboring atoms. When the kinetic energy of the electron is large, that is, well above the edge, single scattering (SS) events usually dominate, as the scattering cross section of the photoelectron is small. This region is called the extended X-ray absorption fine structure (EXAFS) region and it delivers information about coordination numbers and the distance of the nearest neighbors to the absorbing atom. In contrast, at low photoelectron energies (<50 eV above the edge) contained within the X-ray absorption near-edge structure (XANES) region, resonances arise primarily from the interference of scattering pathways between multiple atoms, that is multiple scattering (MS). This region contains information about the three-dimensional structure around the absorbing atom, i.e. coordination numbers, bond distances, and bond angles.

The methodology for time-resolved XAS has been developed at the beginning of the 2000s [8,9,11,23–30]. It generally consists of an optical pump/X-ray probe experiment operating in a transient absorption geometry, where the laser-induced changes in the sample X-ray absorption coefficient are probed by the X-ray pulse as a function of energy and time delay with respect to the laser pulse. In most cases, the X-ray absorption-induced changes are recorded on a pulse-to-pulse basis with the X-ray transmission through the sample being recorded at twice the repetition rate of the laser [26,31]. In such cases the laser pulse is from an amplified femtosecond system operating at 1 kHz, in order to ensure a high photolysis yield, and the X-ray synchrotron pulses (typically 50–100 ps long) are recorded at a repetition rate of 2 kHz. This implies a significant loss of X-ray flux since synchrotrons operate at MHz repetition rates. In recent years the methodology for time-resolved XAS studies has seen significant developments in both temporal resolution and signal-to-noise ratio (S/N). In particular, the implementation of the slicing scheme [32] has made it possible to demonstrate femtosecond XAS of photoexcited species in solutions [33–36]. In addition, a scheme using a high-repetition rate pump laser, operating at an integer fraction of that of the storage ring [37–39], has allowed exploitation of up to two orders of magnitude more X-ray photons than previous schemes based on the use of kHz lasers for picosecond (ps) XAS experiments. Consequently this has led to over an order of magnitude increase of S/N compared to the previous schemes. Finally, the advent of the X-ray free electron lasers (X-FELs) is opening new opportunities in the area of structural dynamics [40–42], as X-FELs have a 10 orders of magnitude larger flux per pulse, compared to the slicing scheme at comparable temporal resolution.

The complex mechanism behind the origin of X-ray absorption spectra means that their analysis is inextricably linked to detailed theoretical simulations, traditionally performed using MS theory within the limits of the muffin-tin (MT) potential [3]. This approach is computationally very efficient and sufficient when the photoelectron is not sensitive to the details of the potential near the ionization limit. However, the limitation of the MT approximation close to the edge means that such calculations cannot always interpret the entire spectrum, particularly the near-edge region. The above experimental developments as well as continuous improvements in the instrumentation are enhancing the sensitivity of both static and time-resolved XAS experiments, thanks to which finer details of the spectra are uncovered. This calls for more detailed theoretical approaches and the last decade has witnessed significant developments, in particular for the simulation of X-ray absorption spectra beyond the MT potential. These include traditional electronic structure methods extended to core hole excitations [43–45]. In addition, there has been extensive work to move beyond the quasi-particle approximation (QPA), which treats the excited electron as a single particle moving in an average potential. Many-body effects, which arise from the breakdown of this approximation, such as the *intrinsic* and *extrinsic* losses [3], have until

recently been accounted for using a phenomenological broadening of the calculated spectrum [46].

There are already several excellent reviews on both static and time-resolved X-ray absorption spectroscopy [1–3,5–9,11,23,28–30,45]. Therefore, here we focus on the most recent experimental developments and the various state-of-the-art theoretical tools for static and time-resolved XAS of species in solution. This chapter is organized in the following way: In the first section, we recall the basic aspects and recent developments of the XAS methodology. This is followed by a detailed summary of the theoretical approaches for simulating X-ray absorption spectra, before finally presenting some recent highlights.

II. EXPERIMENTAL METHODS

The measurement and analysis of X-ray absorption fine structure (XAFS) data are a significant challenge [2,47] and therefore an effective analysis requires a detailed attention to possible systematic errors. Experimentally this type of spectrum can be realized in several ways, each with its own advantages and disadvantages. In the following sections, the two most commonly used detection methods are discussed, followed by their extension into the time domain.

A. Steady-State XAS

1. Transmission and Fluorescence Detection Modes

The simplest and most common method of measuring the X-ray absorption coefficient is X-ray transmission. Using a tunable monochromatic X-ray beam ($\Delta E/E \sim 0.015\%$) both the transmitted (I_t) and incident (I_0) X-ray signals are measured as a function of incident photon energy [1–3,29,30]. These signals are often measured with ion chambers, where the gas mixture can be varied to maintain detector linearity, or with diodes. The X-ray linear absorption coefficient $\mu(E)$ (in cm^{-1}) is then derived from the Lambert–Beer law:

$$A(E) = \mu(E) \cdot d = \ln\left(\frac{I_t}{I_0}\right) \tag{1}$$

where d represents the sample thickness. In principle, $\mu(E)$ refers to the total absorption coefficient of the sample, which includes not only the absorber atom but also the environment in which the absorber is contained, along with coherent inelastic Compton scattering.

In contrast, it is sometimes advantageous to measure $\mu(E)$ by monitoring processes that are proportional to the absorption coefficient, such as the X-ray total fluorescence yield (TFY) or the total (Auger) electron signal emitted by the

sample [49]. These are particularly useful when the signal of interest contributes only a small fraction to the total absorption, or when the sample transmission is very large. The fluorescence and Auger signals are due to the absorbing atom only, and in a careful geometrical arrangement, the elastically scattered photons can be discriminated against resulting in a close to background-free measurement. Photon-counting detectors, such as avalanche photodiodes (APD) or photomultiplier tubes (PMT), are often used. If energy-resolving detectors are used (e.g., silicon drift detectors) the elastically scattered photons, which are of higher energy than the fluorescence photons, can be discriminated against improving the sensitivity of the measurement even further.

For fluorescence yield detection, the measured signal, I_f, is proportional to the absorption coefficient $\mu(E)$, but needs to be corrected for the fluorescence quantum efficiency and geometrical factors. As depicted in Fig. 1, the fluorescence yield is proportional to the X-ray intensity I at the point of absorption and the fluorescence efficiency ϵ_A. Therefore, given a measured fluorescence flux at position y, the signal is given by

$$I_f = I_0 \mu_A(E) \epsilon_A \cdot e^{-\mu(E)y} \cdot e^{-\mu(E_f)z} \tag{2}$$

where $\mu_A(E)$ is the absorption coefficient of the absorbing atom, z is the escape depth, $\mu(E)$ is the total absorption coefficient including the environment around the absorbing atom, E is the photon energy of the incident beam, and E_f is the

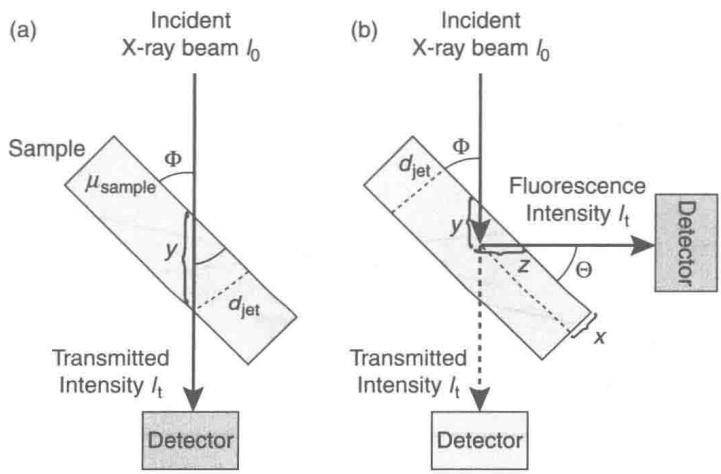

Figure 1. The two most commonly used experimental configurations for measuring XAS are (**a**) transmission and (**b**) fluorescence yield modes. Figure from Ref. [48].

emission energy of the fluoresced photon. After integration over y and z and using the geometry shown in Fig. 1 ($\Phi = \Theta = 45°$) [48], one arrives at

$$I_f = \frac{I_0 \mu_A(E) \epsilon_A}{\mu(E) + \mu(E_f)} \left(1 - e^{-[\mu(E)+\mu(E_f)]d'}\right) \tag{3}$$

where $d' = d/\sin(45°)$. The fluorescence intensity is thus directly proportional to the absorption coefficient of the absorber, but in addition, the geometrical factors and the quantum efficiency are now included. The above equation can be further approximated in two different experimental limits: the thick-sample [49] and the thin-sample [50] limits. However in both cases, the resulting X-ray fluorescence can be directly related to the changes in the absorption coefficient of the central absorbing atom and thus it should yield quantitatively the same XAS spectrum, as recorded by X-ray transmission [51].

In general X-ray signals are normalized such that the signal well before the absorption edge is set to zero and the post-edge signal is set to 1. This allows more straightforward analysis and comparisons of signals across experiments and to theory. All X-ray signals presented in this chapter are normalized this way.

B. Time-Resolved XAS

1. General Setup

Time-resolved XAS experiments are implemented within the laser-pump/X-ray-probe scheme, for which a generalized setup is shown in Fig. 2. Here, an ultrashort laser pulse starts a chemical reaction and a delayed X-ray pulse probes the changes induced in the system by the photoexcitation. The detected transient XAS signals

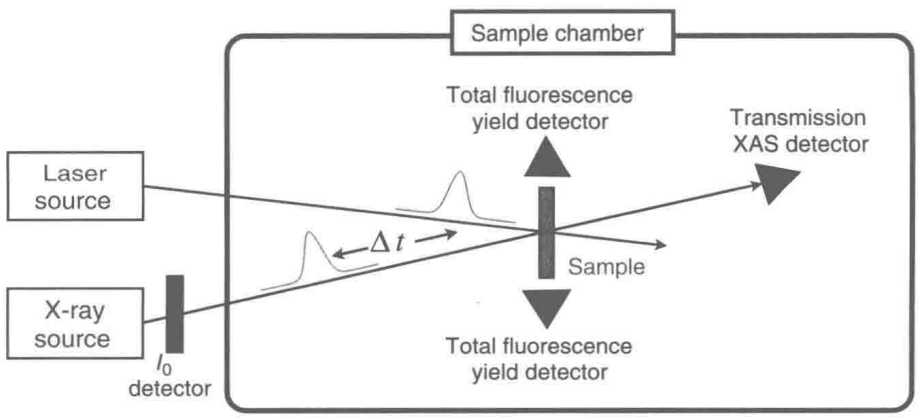

Figure 2. Sketch of the time-resolved XAS setup for the study of liquid samples. The continuously refreshed sample can be a flow capillary, a flow-cell, or a high-speed liquid jet. (See the color version of this figure in Color Plates section.)

will contain all the photoinduced electronic and structural changes between the ground state spectrum and the excited state spectrum. However, the use of an X-ray probe in contrast to an optical probe introduces some specific conditions [8,25,31]. These are as follows:

- An X-ray pulse contains $\sim 10^4 - 10^6$ photons, much less than a typical ultrashort laser pulse that can contain $> 10^9$ photons nJ^{-1}. This necessitates an optimization of the sample and the detection system to minimize the number of X-ray photons required to measure a given X-ray absorption cross section with the highest possible accuracy, thus maximizing the S/N [8,28]. The closer the measurement to the shot-noise limit, the more efficiently it can detect small XAS changes.
- *The Absorption Cross Section of X-rays.* Hard X-ray absorption cross sections are typically two to four orders of magnitude smaller than optical cross sections; therefore, the interaction of the sample with the X-ray probe pulse is weak, yielding small X-ray signal changes. Conversely the optical density (OD) of the sample at visible wavelengths is often quite high, resulting in a significant difference between the laser and the X-ray absorption that is far from ideal. Maintaining a balance between the maximum possible X-ray absorption and an optical density that will absorb 90% of the laser photons can be challenging since external factors, like sample solubility, can also affect the conditions.
- To ensure that the X-rays are probing the photoexcited region of the sample they need to be focused to a spot size smaller than that of the laser focus. The laser focus size determines the excitation fluence (mJ cm^{-2}), which is related to the population of the excited state. At typical third-generation bend magnet beamlines, X-ray foci are in the 100–300 μm diameter range. The divergence of the X-ray beam is inherent to the source properties and limits its brilliance. This generally restricts the experiment to a large laser spot size, which requires high pulse energies to maintain sufficient fluence and places limitations on the laser sources used for the experiments. An alternative approach, which is available at some insertion-device (wiggler, undulator) beamlines at third-generation synchrotrons, is to use specialized X-ray optics, for example, Kirkpatrick–Baez focusing mirrors [52–55] or zone plates [56,57], which can significantly reduce the X-ray focal size down to the 1–10 μm range. This allows the use of more diverse laser sources and wavelengths.
- The typical X-ray flux available at a third-generation synchrotron is composed of a train of X-rays pulses (the multibunch, Fig. 3), generally separated by a few nanoseconds (ns). In order to perform pump–probe measurements, an isolated probe pulse must be used. The approach taken by many light sources is to place an isolated electron bunch into the ion-clearing gap of the

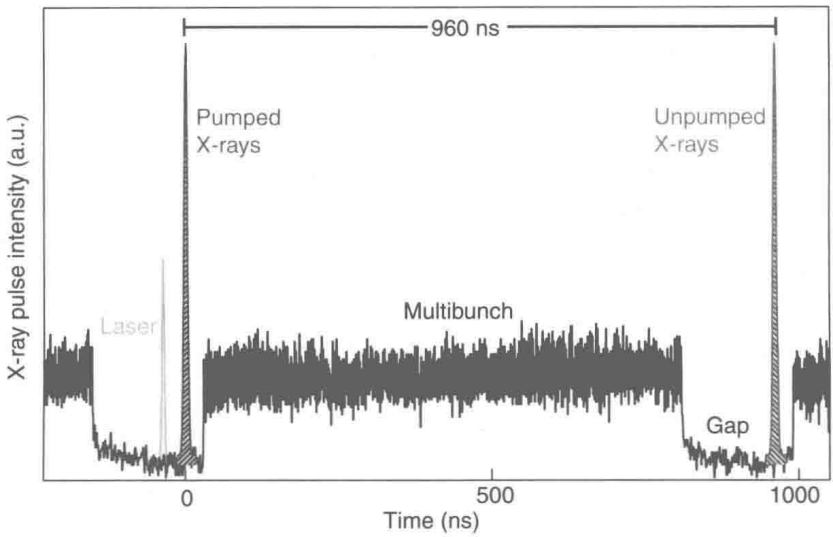

Figure 3. Plot of the X-ray fill pattern at the Swiss Light Source showing the isolated hybrid pulse, the photo excitation laser pulse, the multibunch pulse train, and the ion-clearing gap. (See the color version of this figure in Color Plates section.)

fill pattern (Fig. 3). This gap is typically ~200 ns long so with fast X-ray detectors, such as APDs or PMTs, it is possible to measure only the X-ray pulse from this isolated bunch (so called *hybrid pulse*), allowing a pump–probe experiment to achieve a time resolution limited by the duration of this X-ray pulse (~50–100 ps).

Data acquisition of time-resolved XAS signals is based on the measurement of transient absorption spectra, which is the difference between the absorption of the excited sample minus that of the unexcited sample. Briefly, the XAS signal at a specific X-ray energy and pump–probe time delay is recorded at twice the laser repetition rate, alternating between the signal from the excited sample (pumped) and that from the unexcited sample (unpumped). At the Swiss Light Source (SLS) synchrotron (Villigen, Switzerland), the pulse is delivered at a repetition rate of 1.04 MHz. In addition, a zero measurement is made for every X-ray measurement by reading the detector signal in the gap where no X-rays are present. This electronic zero level is then subtracted off the corresponding X-ray signal to compensate for any drifts over time of the data acquisition baseline. The signals provided to the user correspond to the pumped XAS signal ($I_p = [I_p]^{X\text{-ray}} - [I_p]^{zero}$), the unpumped XAS signal ($I_{unp} = [I_{unp}]^{X\text{-ray}} - [I_{unp}]^{zero}$) and the pulse-to-pulse difference signal of pumped–unpumped with the zeros being ignored as the electronic baseline will have no time to drift during the interval separating the two X-ray measurements ($I_{diff} = [I_p]^{X\text{-ray}} - [I_{unp}]^{X\text{-ray}}$). The reported measurements